Hall Photovoltage Imaging of the Edge of a Quantum Hall Device

A. A. Shashkin,* A. J. Kent, J. R. Owers-Bradley, A. J. Cross, P. Hawker, and M. Henini
Department of Physics, University of Nottingham, University Park, Nottingham NG7 2RD, United Kingdom
(Received 14 March 1997)

We report experiments using a Hall photovoltage imaging technique with a resolution of better than 5 μm to visualize the potential profile in a standard Hall bar device at low temperature and in high magnetic fields. The images show the potential rises sharply close to the device edges and is flat in the bulk. We obtain the characteristic length scale of the edge confining potential as 10 μm in our devices. This measurement enables the determination of the contribution of the edge current to the total Hall current. We also give a qualitative account of the origin of the photovoltage in the quantum Hall effect. [S0031-9007(97)04831-X]

PACS numbers: 73.40.Hm, 73.50.Pz

In a magnetically quantized two dimensional electron gas (2DEG), the Landau levels bend up at the sample edges due to the confining potential, and edge channels are formed where these intersect the Fermi energy. These edge channels can play a significant role in determining the electrical transport properties of quantum Hall devices [1]. Much experimental work has been done with the aim of understanding the dynamics of the edge electrons. However, to date there has been no direct experimental evidence for the predicted edge channel structure nor has the current distribution in the 2DEG been visualized. Magnetotransport studies which test average characteristics of a sample provide only a crude estimation of the "width" of the edge region which seems to extend for ≥ 1 μm into the bulk [2,3], implying that the edge confining potential is "soft" in real samples.

Direct verification of the edge channel picture may be obtained by using imaging techniques similar to those of Refs. [4–6], which are sensitive to the potential profile within the sample. Owing to limitations in the spatial resolution of the early experiments it was not possible to see any detailed structure in the potential profile near the sample edges. An attempt to overcome this problem by artificially creating a gradient in the 2D electron density to spread out the "edge channels" was made in [7]. However, the features interpreted as edge channels in [7] can also be related to the phenomenon of Hall current pinch [8–10]. That is, the 2D electron density gradient results in a strongly inhomogeneous current distribution over the bulk of the sample and the Hall current flows in narrow strips defined by the minima of conductivity σ_{xx}. In fact, the pinch of Hall current cannot simulate edge channels for two reasons: (i) this bulk effect is not related to the edge at all and will occur in an infinitely large sample; and (ii) the 2D electron density gradients achieved in [7] are about 3 orders of magnitude smaller than those expected at the sample edge. Therefore, information about *edge* states can be obtained on standard samples only by improving the resolution of the detection technique. Here we use a Hall photovoltage imaging experiment with an optical resolution of 5 μm to study the potential profile in a standard Hall bar sample. We visualize the edge regions in 2D images and determine the scale of confining potential ≈ 10 μm.

The samples were based on a near surface GaAs/AlGaAs heterojunction in which the doping and the width of the doped layer are kept small. As a result the samples were free of a parallel conducting channel even under direct illumination, and there were no persistent photoconductivity effects. The 2DEG density and 4.2 K mobility were 4.4×10^{15} m^{-2} and 100 m^2 V^{-1} s^{-1}, respectively. A Hall bar, 1.2 mm long by 98 μm wide, was defined by etching the layers, and there were a total of 10 contacts made: a current contact at each end and four voltage probes on each side; the center pair of probes on each edge were separated by 400 μm and the others by 200 μm. The device was mounted on a copper rod attached to the mixing chamber of a dilution refrigerator. A magnetic field of up to 12 T could be applied perpendicular to the sample by means of a superconducting solenoid. Quartz windows were fitted in the vacuum cans and radiation shields to permit direct optical access to the sample. Outside of the cryostat there was mounted an optical system capable of focusing the beam from an Ar^+ laser to a diffraction limited spot on the top surface of the sample. The spot size was determined by independent measurement to be 5 μm across. The spot could be positioned on the sample with submicron accuracy by means of a pair of galvanometer-controlled scanning mirrors (see Fig. 1). The average laser power reaching the sample was estimated to be of the order 1 nW which was within the linear regime of the 2DEG response. The laser beam was chopped at a frequency of 6 kHz by means of an acousto-optic modulator, and the induced photovoltage in the sample was measured using a lock-in amplifier. In this study there was no dc bias current through the sample.

The samples were carefully selected by using the imaging technique to find macroscopically homogeneous ones. It is interesting to note that many of the inhomogeneous samples show quite good magnetotransport characteristics. Typical traces of the magnetoresistances ρ_{xx} and

 0031-9007/97/79(25)/5114(4)$10.00 © 1997 The American Physical Society

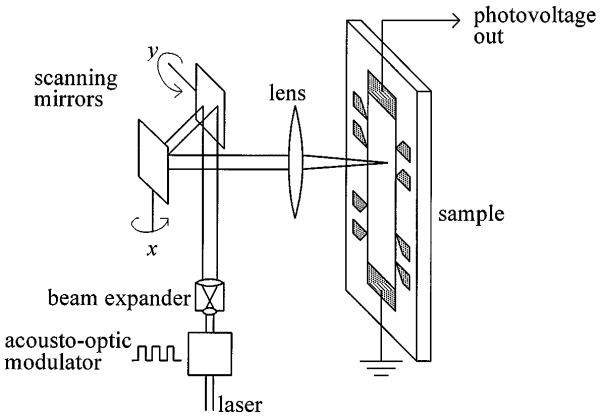

FIG. 1. Schematic diagram of the photovoltage imaging system.

ρ_{xy} for our devices are displayed in Fig. 2. The absence of parallel conduction is indicated by zeros in the resistance ρ_{xx} as seen from the figure.

Figure 3 shows an image of the Hall photovoltage at filling factor $\nu = 2$. It was taken in the middle part of the device using the current contacts at the ends of the Hall bar. Also shown is a line scan taken horizontally through the image. We observe a strong response when illuminating near the edges of the sample. In the bulk of the device, where the Landau levels are flat, the response is very small. The polarity of the response is different on opposite edges and reverses upon reversal of the magnetic field. This undoubtedly points to the Hall origin of the observed photovoltage. As seen from Fig 3, the photovoltage does not depend on the coordinate along the sample, except in the near vicinities of the side contacts. The half width of the observed lines is 10 μm which is wider than the probe beam, and the positive and negative peaks at each edge are separated by 84 μm which also indicates a relatively wide responsive region. The image at filling factor $\nu = 4$ is basically the same except that the amplitude of the edge response is reduced by half. Thus, one can conclude that the photovoltage is proportional to the magnetic field B.

We explain the origin of a Hall photovoltage as follows: The laser light incident on the sample induces photocarriers, thereby slightly increasing the 2DEG density locally. When illuminating near the edge of the sample the photoinduced electrons diffuse at the Fermi level, E_F, to the opposite edge; i.e., the average diffusion current is directed to the opposite edge. In the absence of magnetic field this would be stopped by an arising potential difference according to the Einstein relation. In the quantum Hall effect, when the diagonal conductivity is negligible compared to the Hall conductivity, it is the Hall current in the Landau levels below E_F [11] that balances the diffusion current. The balancing Hall current leads to the appearance of a Hall potential difference along the device while the net current through the sample is equal to zero. This interpretation gives the correct sign and magnetic field dependence of the observed photovoltage. The amplitude of the photoresponse is proportional to the value of diffusion current and so to the gradient

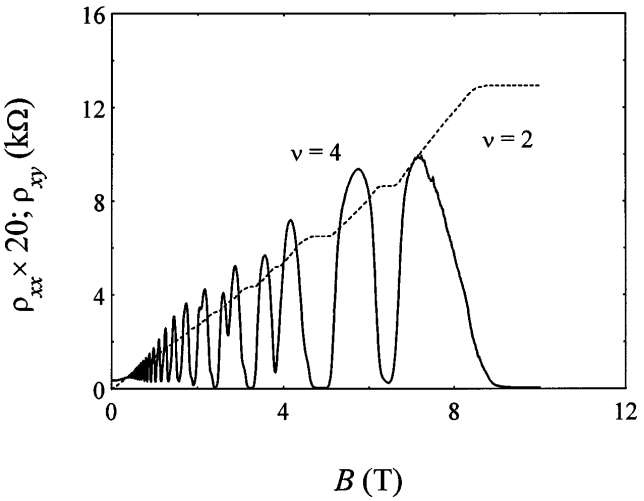

FIG. 2. Magnetotransport characteristics of the device under constant illumination.

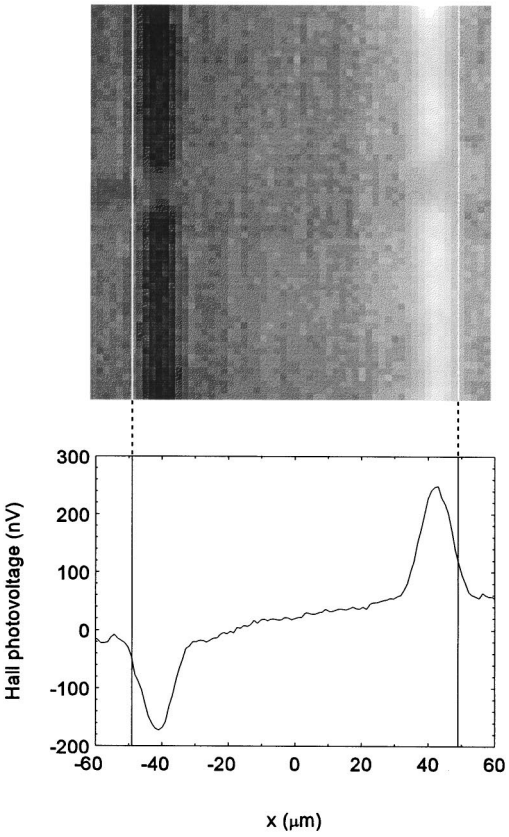

FIG. 3. Image of the Hall photovoltage at $\nu = 2$. The image covers an area of 120 × 120 μm, and the pixel size is 2 μm. Also shown is a line scan taken horizontally through the image at $\nu = 2$ and 4.

of the photoinduced electron density, which itself depends on the rate of the spatial separation of photoinduced carriers. The small response from the bulk of the device (Fig. 3) indicates that the diffusion of photoexcited electrons at the Fermi energy is slow so that the carriers are not spatially separated. The strong response seen when illuminating at the sample edges is due to separation of the photoinduced carriers by the confining potential. Since the diffusion coefficient is expected to be proportional to the conductivity σ_{xx}, one can trace the behavior of the images at different diffusion rates by varying the magnetic field and temperature. We find that at conductivities $\sigma_{xx} \gg \sigma^* = 10^{-8}\ \Omega^{-1}$ the peaks in Fig. 3 broaden and spread out into the bulk, smearing the flat region. In the opposite limit, when σ_{xx} vanishes, the response tends to zero with no change in the linewidth; i.e., the diffusion current is blocked by the poorly conducting bulk of the 2DEG. The images presented correspond to the empirically determined optimum condition, $\sigma_{xx} \sim \sigma^*$, to attain the narrowest lines and maximum response from the edges. The images remain very similar when the temperature is decreased from 1.5 K down to about 0.2 K with the simultaneous tuning of magnetic field to keep $\sigma_{xx} \sim \sigma^*$. We have checked that (i) the reduction of light intensity does not affect the observed results (i.e., that it is within the linear regime) while at higher light intensities the probe enlarges and the resolution becomes worse; (ii) when defocusing the optical system the images do not change appreciably over a wide range of lens positions until the probe size becomes comparable to the dimension of the structures observed. We note that the fine structure due to individual edge channels discussed in [12] is not seen in our experiments. The most likely reason for this is that the ultimate resolution of the imaging technique is still not sufficiently high.

It was possible to move the probe spot in sub-μm steps, so we attempted to improve the effective resolution by deconvolving the images with a point-spread function corresponding to the known laser spot size and intensity profile. We found that the signal-to-noise ratio of the results was not good enough for us to establish the presence of a fine structure in the images. In particular, we found that the confining potential can be quite adequately described by a linear function. Assuming that this is the case, we obtain that the edge region is about 10 μm wide. This result allows us to estimate the edge contribution to the total current in our samples as the ratio of the edge region dimension to the sample width, regarding the Hall electric field to be uniform. The large scale of the confining potential is likely to be due to the fabrication process of standard Hall devices: Both charged impurities present on the mesa boundary and the presence of the mesa boundary itself may result in depleting the 2DEG at the edges. Since the screening of in-plane electric fields by the 2DEG is rather poor, the depletion region can extend a large distance from the edge. Thus, we expect that the obtained confining potential scale is not universal: For gated samples, for instance, it should be smaller, taking into account the gate screening.

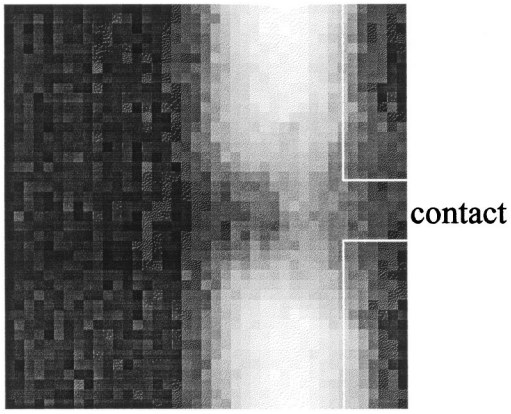

FIG. 4. Close-up view of the side-contact region. The end (current) contacts are used for the measurement.

Figure 4 shows a detailed image of the side contact region seen in Fig. 3. The presence of a contact modifies the confining potential locally: We see that the response gets smaller in the region of the sidearm and is displaced towards the contact. Because the contact width is less than the confining potential scale, obviously the 2DEG density in the sidearm should be depleted. This leads to a finite slope of the potential profile along the center line of the sidearm region as compared to a wide contact for which the response away from the edges in the contact region is expected to vanish.

Another test to verify the proposed model for the Hall photovoltage has been done by taking the measurement

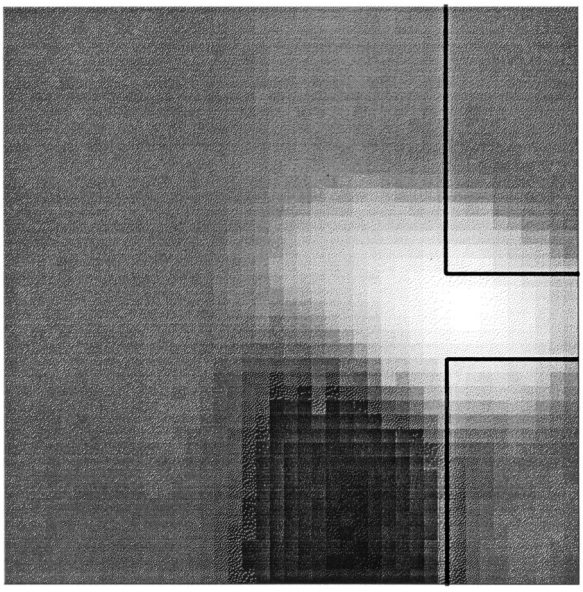

FIG. 5. Close-up view of a side-contact region; the side (potential probe) contact and the top (current) contact are used for the measurement.

using the side contact and one of the current contacts at the end. In this case, at the same light intensity, the response is much larger and the picture changes significantly; cf. Figs. 4 and 5. In the arrangement of Fig. 5 the sample edges "converge" in the region of the sidearm and, as a result, the Hall photovoltage changes its polarity over a much shorter distance, of order the width of the sidearm (see Fig. 5). The magnitude of the response becomes larger because the photoexcited carriers now have to diffuse a much shorter distance to reach the other "edge."

In summary, we have made high resolution Hall photovoltage images of the potential profile in a standard Hall bar. The origin of the photoresponse in the quantum Hall effect as well as the behavior of the images when varying the magnetic field and temperature have been explained. We determine the length scale of the edge confining potential as 10 μm, which allows us to estimate the edge contribution to the total current in our samples at $\approx 20\%$.

The authors acknowledge the financial support for this work from the European Union and the Department of Physics at the University of Nottingham.

*Permanent address: Institute of Solid-State Physics, Chernogolvka, 142432 Russia.

[1] M. Büttiker, Phys. Rev. B **38**, 9375 (1988).
[2] N. B. Zhitenev, R. J. Haug, K. von Klitzing, and K. Eberl, Phys. Rev. Lett. **71**, 2292 (1993).
[3] S. Takaoka, K. Oto, H. Kurimoto, K. Murase, K. Gamo, and S. Nishi, Phys. Rev. Lett. **72**, 3080 (1994).
[4] A. J. Kent, D. J. McKitterick, L. J. Challis, P. Hawker, C. J. Mellor, and M. Henini, Phys. Rev. Lett. **69**, 1684 (1992).
[5] A. A. Shashkin, A. J. Kent, P. Harrison, K. R. Strickland, L. Eaves, and M. Henini, Semicond. Sci. Technol. **9**, 2110 (1994); A. A. Shashkin, A. J. Kent, P. Harrison, L. Eaves, and M. Henini, Phys. Rev. B **49**, 5379 (1994).
[6] P. F. Fontein, J. A. Klienen, P. Hendiiks, F. A. P. Blom, J. H. Wolter, H. G. M. Lochs, F. A. J. M. Driessen, L. J. Giling, and C. W. J. Beenakker, Phys. Rev. B **43**, 12 090 (1991).
[7] R. J. F. van Haren, F. A. P. Blom, and J. H. Wolter, Phys. Rev. Lett. **74**, 1198 (1995).
[8] G. Ebert, K. von Klitzing, and G. Weimann, J. Phys. C **18**, L257 (1985).
[9] V. M. Pudalov and S. G. Semenchinskii, Pis'ma Zh. Eksp. Teor. Fiz. **42**, 188 (1985) [JETP Lett. **42**, 232 (1985)].
[10] A. A. Shaskin, V. T. Dolgopolov, and S. I. Dorozhkin, Zh. Eksp. Teor. Fiz. **91**, 1897 (1986) [Sov. Phys. JETP **64**, 1124 (1986)].
[11] V. T. Dolgopolov, G. V. Kravchenko, and A. A. Shashkin, Solid State Commun. **78**, 999 (1991).
[12] D. B. Chklovskii, B. I. Shklovskii, and L. I. Glazman, Phys. Rev. B **46**, 4026 (1992).